Key role of anionic doping for H_2 production from formic acid on Pd(111)

Pei Wang[†,‡,⊥], Stephan N. Steinmann[‡,⊥], Gang Fu[*,†], Carine Michel[‡] and Philippe Sautet[*,‡,§]

† State Key Laboratory for Physical Chemistry of Solid Surfaces, Institution College of Chemistry and Chemical Engineering, Xiamen University, Xiamen 361005 (China)

‡ Univ Lyon, Ens de Lyon, CNRS UMR 5182, Université Claude Bernard Lyon 1, Laboratoire de Chimie, F69342, Lyon, France

§ Department of Chemical and Biomolecular engineering, University of California, Los Angeles, Los Angeles, CA 90095, United States

ABSTRACT: Hydrogen evolution by the catalytic decomposition of formic acid in solution is a key reaction for hydrogen storage for which palladium is one of the most efficient catalysts. Based on DFT computations, we explain why the presence of an anionic promoter renders palladium more active and more selective for formic acid dehydrogenation. The promotion is well captured by modelling the anion by a negatively charged surface. This promotional effect can be traced back to the modulation of the electric field at the catalyst surface, with a strongly contrasted action on the energy of the various species along the competing pathways through the electrostatic interaction between the electric field and the surface dipole moment. As a result, both the reaction kinetics and selectivity are markedly improved. This opens the door to a rational design of catalytic systems using promoters.

The transformation of formic acid in solution into CO_2 and H_2 is a key reaction for safe intermittent hydrogen storage and utilization in energy applications, especially for fuel cells.[1] Transition metal (TM) catalysts, particularly Pd, show a good activity for this catalytic decomposition.[2] Unfortunately, the dehydrogenation reaction is usually in competition with the dehydration, generating H_2O and CO. For practical use, the dehydration process should be avoided since CO binds very strongly to the late TMs and thus acts as a poison for the Pt catalyst in the "downstream" H_2 electro-oxidation.[2]

If TM catalysts already show a fair activity, the presence of sodium formate HCOONa can strongly increase the rate of hydrogen production (by a factor of ~30).[3]-[6] In electrochemical conditions, the formic acid oxidation is also promoted by adding sodium formate,[7]-[9] and more generally anions, like sulfate or acetate.[10] In both cases, the origin of the promoting effect is still unclear, hampering the rational design of a promoted catalytic process.

The nature of the surface intermediates and the reaction mechanism are the keys to reach a molecular scale understanding of this reaction. Experimentally, formate species, (HCOO, bound in a bidentate or monodentate manner on the TM surface) have been evidenced by IR spectroscopy.[11]-[13] In particular, the role of bidentate formate is unclear, since it has been considered as a reactive species along the pathway,[3],[13],[14],[15] or, in contrast, as a (blocking) spectator.[7][16],[17] Even the nature of the surface formate is unclear, since it can be a radical derived from the homolytic dissociative adsorption of formic acid or an anion (HCOO⁻) – cation pair from solution.

Modeling is a powerful tool to provide a better understanding of catalytic systems.[18],[19] The effect of metallic alkali promoters on the dissociation of N_2 on Ru(0001) was related to an electrostatic effect by Nørskov and co-workers.[20],[21] However, here, the promoter is not a metallic alkali in gas-phase but an alkali salt in solution. We report how and why sodium formate promotes the reactivity and selectivity towards H_2 production from formic acid. Computations are based on periodic Density Functional Theory (DFT) with a generalized gradient functional (PBE) (see SI for more details). The solvent is described by a continuum model,[22] and the simulation cells of charged surfaces are neutralized through an idealized counter ion distribution representative of a 1 M electrolyte.[23],[24]

According to the accepted terminology,[14],[15] two pathways are distinguished for dehydrogenation based on their intermediate: the formate and carboxyl pathways, represented in Scheme 1, together with the undesired dehydration pathway. In the following notation, the underlined atoms form a chemical bond with the surface or point towards the surface. As shown in Scheme 1, the decomposition of formic acid could be initiated by O-H bond breaking from HCO<u>OH</u> (O-H down configuration), or C-H bond breaking from <u>H</u>COOH (C-H down configuration). Alternatively, <u>H</u>CO<u>OH</u> (C-H, O-H down configuration) could serve as the direct precursor for these two pathways.
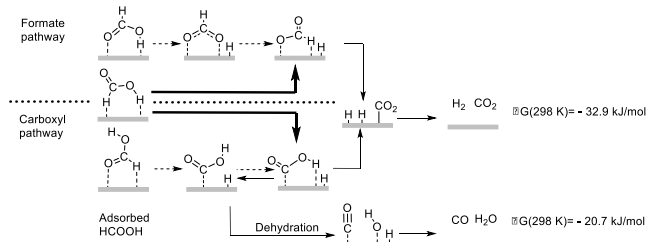
Scheme 1. Mechanisms for formic acid decomposition, including the dehydrogenation through the formate and the carboxyl pathway together with its dehydration branch to CO. For simplicity, the Pd(111) surface is indicated by a grey line.

Table 1 summarizes the effective barriers for each pathway, which are conveniently described by their energetic spans.[25] In the formate pathway, HC$\underline{OO}$$\underline{H}$ undergoes O-H bond activation to produce bidentate HC$\underline{OO}$, followed by a rotation to give monodentate $\underline{H}$COO,[26],[27] which then yields CO_2 and an adsorbed H atom. Alternatively, the monodentate $\underline{H}$COO can be generated directly from chemisorbed HCO$\underline{OH}$, bypassing the bidentate adsorption mode and the required re-orientation. The Gibbs free energy profiles for the two pathways are given in the left part of Figure 1. We find that in the absence of a promoter (red line), the indirect pathway through bidentate formate is clearly preferred over the direct counterpart. If the bidentate formate HC$\underline{OO}$ (-0.27 eV) is easily generated, its reorientation into the reactive monodentate $\underline{H}$COO involves a large barrier of 0.94 eV, which induces a high energetic span (1.42 eV). However, the monodentate $\underline{H}$COO seems to be inaccessible directly, with an unstable $\underline{H}$COO$\underline{H}$ precursor (+0.34 eV) and a high lying transition state (TS) for its direct formation (TS-f$_{d0H}$, +0.98 eV). It is important to underline here that the "HCOO" units created along the decomposition of HCOOH, together with adsorbed H are formally neutral species, without generation of excess charge on the metal surface.

Table 1. Gibbs free energetic span (δG_{span}, in eV, at 303 K) of the formate pathway, the carboxyl pathway and the dehydration pathway shown in Scheme 1 as a function of the promoter model.

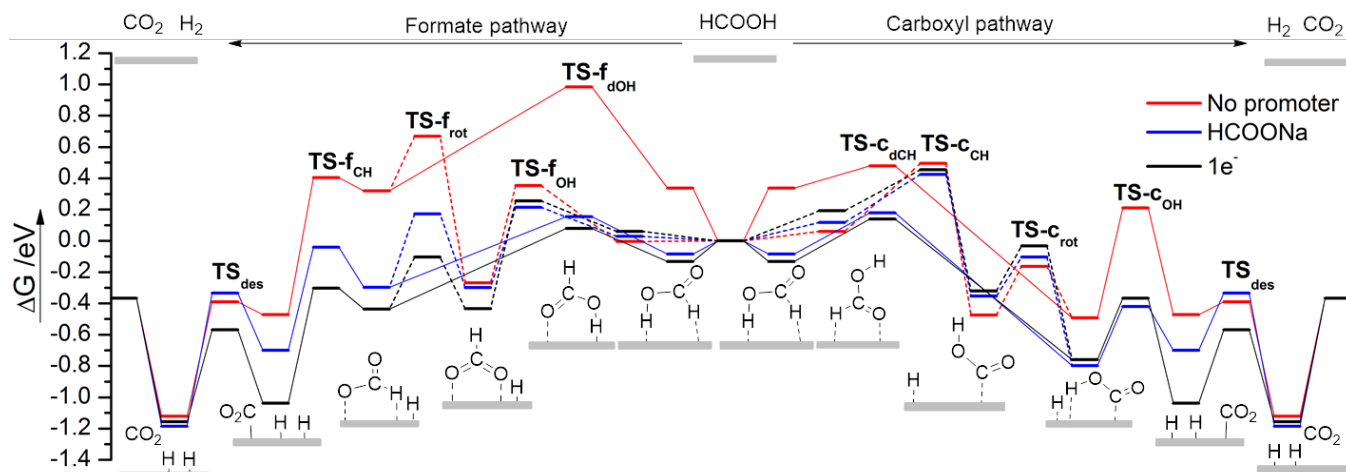| Pathway	No promoter	HCOONa	HCOO	HCOO$^-$	1e$^-$
Formate	1.42	0.95	1.51	0.99	0.87
Carboxyl	1.23	0.96	1.17	0.99	0.94
Dehydration	1.65	1.78	1.79	1.90	1.67

In the carboxyl pathway, the C-H bond cleavage precedes the O-H bond breaking, passing through a carboxyl intermediate (right part in Figure 1). Similar to the formate pathway, two carboxyl configurations are possible, the H-up (C$\underline{OO}$H) and the H-down (C$\underline{OO}$$\underline{H}$) configuration, the latter being the reactive one to yield CO_2. Thus, we subdivide the carboxyl pathway into a direct and an indirect mechanism for the formation of the H-down configuration (C$\underline{OO}$$\underline{H}$). Since the corresponding C-H scission transition states are lying almost at the same energy, the distinction is not crucial in the absence of a promoter, but it will become essential in its presence. When the weakly adsorbed

HC$\underline{OO}$$\underline{H}$ serves as the precursor, the carboxyl intermediate C$\underline{OO}$$\underline{H}$ can be directly formed, which is followed by the O-H bond cleavage to generate CO_2 plus H_2. Alternatively, the carboxyl pathway can proceed from the more stable HC$\underline{OO}$$\underline{H}$ mode, leading to another carboxyl conformer C$\underline{OO}$H. From this key intermediate, two routes are branching. On one hand, C$\underline{OO}$H undergoes O-H bond rotation to give C$\underline{OO}$$\underline{H}$, which produces the dehydrogenation products. On the other hand, the breaking of C-O bond in C$\underline{OO}$H yields the dehydration products; CO and H_2O (see Figure S3 for the corresponding profile). The energetic span for dehydration is very high (1.65 eV) and defined by the C-H and C-O scission TS (all lying at ~0.5 eV) on one hand and the chemisorbed CO on the other. While sharing the same limiting TS (C-H scission) the dehydrogenation is easier (δG_{span} = 1.23 eV) since the product is less strongly bound (2H vs. CO).

To sum up, in solution and in the absence of a promoter, the main route on Pd(111) is the dehydrogenation following the carboxyl path. Unfortunately, the C$\underline{OO}$H intermediate is also the precursor for C-O dissociation and hence can open the door to undesired traces of CO, since the gap between TS-c$_{OH}$ (0.21 eV) and TS-c$_{CO}$ (0.49 eV) is not very large.

Let us now turn to the influence of HCOONa. This salt is dissociated in a heterolytic way at the Pd/water interface, yielding a chemisorbed bidentate anionic formate HCOO$^-$ and a hydrated Na$^+$ cation (+0.97 a.u. from bader charge analysis) at around 4 Å distance from the surface. The main influence of HCOONa is to considerably promote the formate pathway, drastically reducing its energetic span from 1.42 to 0.95 eV due to a strong stabilization (0.62 eV) of the monodentate $\underline{H}$COO along the path (blue line in Figure 1). The co-adsorbed HCOONa does not affect the bidentate HC$\underline{OO}$, so that the two forms of formate become isoenergetic. The rotation barrier is divided by two (from 0.94 to 0.47 eV), facilitating the dehydrogenation from HC$\underline{OO}$. The relative orderings of the adsorption modes of formic acid are also affected by the promoter: HC$\underline{OO}$$\underline{H}$ is now more stable than HC$\underline{OO}$$\underline{H}$. Thus, both the initial and the final state of the direct OH scission are stabilized (Figure 1 left), rationalizing why the related TS-f$_{d0H}$ is markedly lowered (by 0.82 eV) upon co-adsorption of HCOONa. As a consequence, the path that directly goes through the monodentate formate is easier. The carboxyl pathway is also promoted by HCOONa but to a lesser extent, giving an energetic span equivalent to that of the formate path (0.99eV). In other words, those two pathways are energetically equally probable in the presence of a formate anion. Furthermore, since HC$\underline{OO}$$\underline{H}$ and the corresponding TS are stabilized, the promoted carboxyl pathway is also the "direct" one. Concerning the undesirable dehydration process, the TOF limiting TS (TS-c$_{CO}$) is only slightly stabilized (by 0.1 eV) in presence of the promoter, which enlarges the gap (0.81 eV vs. 0.28 eV) between TS-c$_{OH}$ and TS-c$_{CO}$, and thus favors the dehydrogenation from C$\underline{OO}$$\underline{H}$, enhancing the selectivity. In short, HCOONa has a strongly contrasted action on the various species, stabilizing some by 0.8 eV and destabilizing others by 0.1 eV. In the following, we provide a detailed rationalization of this distinct influence and propose a simplified model that

allows assessing these effects without the need for cumbersome co-adsorption computations.

Figure 1. Gibbs free energies reaction profiles (eV) for HCOOH decomposition over Pd(111) via the formate (left) and carboxyl (right) pathway. Pd(111) is modified by various promoter models: No promoter (red line), HCOONa dissociated into HCOO⁻ anion and Na⁺ (blue line), and 1e⁻ added to the surface (black line). The solid lines indicate the direct formate/carboxyl pathway for a given model, while the dot lines represent the indirect pathways.

Given that solvated Na^+ does not strongly interact with the Pd (111) surface, the promotion effect can be attributed to the coadsorption of $HCOO^-$. The working principle of $HCOO^-$ promotion can be further decomposed into the coadsorption of neutral HCOO and the effect of a negative charge. To gain more insight on the promotion mechanism, we consider three models: the co-adsorption of $HCOO^-$ (Figure S1-S3), the co-adsorption of the neutral HCOO (Figure S1-S3) and the reactivity of a negatively charged surface (profiles in black in Figure 1 and S4). From Figure 1, S1-S4 and the energetic spans (Table 1), it is clear that the neutral HCOO co-adsorption behaves closely to the non-promoted situation (red) while the $HCOO^-$ anion and the negatively charged surface (black) both mimic the presence of HCOONa (blue). Hence, the promotion effect originates in the electron donation ability of HCOONa towards the Pd surface.

Having established the equivalence of adsorbing one electron or HCOONa on the surface, we now identify the physical origin of the change in relative energies. The injected charge is localized at the metallic surface layer (Figure S8-S11) and one of the most immediate effects of such a charge injection is the creation of an electric field perpendicular to the surface. This field interacts with surface dipole moments created by the adsorbates.[20][28] The adopted procedure to estimate the electrostatic interaction between the electric field (ℰ) and the dipole (μ) is detailed in the SI (Table S6-S8). Figure 2 plots the adsorption energy relative to the non-promoted condition, $\Delta\Delta G$, against the electrostatic interaction ($E_{dip}= -\mathcal{E}*\mu_z$) for chemisorbed formic acid (H<u>C</u>OO<u>H</u>) and the four key intermediates (<u>C</u>OOH, <u>C</u>OO<u>H</u>, H<u>C</u>OO and H<u>C</u>O<u>O</u>) in the presence of various promoter models. Importantly, the change in adsorption energy, $\Delta\Delta G$, is strongly correlated to the electrostatic interaction energy. Adsorbates inducing a large negative out of plane surface dipole component μ_z (H<u>C</u>OO<u>H</u> in black, H<u>C</u>O<u>O</u> in blue, <u>C</u>OO<u>H</u> in green) are strongly stabilized, while species leading to small (negative or positive) dipole moments

(H<u>C</u>OO and <u>C</u>OOH) are weakly affected. The electrostatic interactions from the HCOONa and formate anion promoters are similar to that of the surface charged by 1 electron, confirming that this simple model is representative of the underlying processes governing the promotion by HCOONa. Although our procedure overestimates the field (the actual field varies over the size of the adsorbate and is counterbalanced by the double layer effect), the strong and common correlation between $\Delta\Delta G$ and E_{dip} identifies the electrostatic interaction as the dominant promotional effect of anions. This explains the experimental results with mixtures of formic acid and sodium formate, and can be readily extended to other electron donor species, like anions or amine ligands.[29]

Still, the difference in energetic span between the non-promoted and the HCOONa assisted pathway (0.3 eV) would be associated with a rate enhancement of ~10⁵ at 300 K, much larger that the observed factor of ~30. In the decomposition of pure formic acid, however, a certain concentration of formate anions is present in the solution (~0.01 M) that will adsorb on the Pd catalyst and self-assist the oxidation of formic acid. This assisting role of solution formate anion species also agrees with the observed increase in catalytic activity of Pd/C with the increase of the pH .[3],[5],[6] Increasing the pH obviously increases the concentration of formate anions, their surface coverage and the amount of injected charge in the Pd particle, hence enhancing the promotional effect. However, the optimal pH cannot be assessed easily based on modelling since it relies also on other experimental aspects such as the nature of the carbonaceous support, the total concentration of HCOOH/HCOONa, etc.

In a nutshell, our study depicts formate as a Janus species in the mechanism, both a promoter anion and a reaction intermediate. On the electron-rich Pd surfaces, bidentate and monodentate HCOO are isoenergetic, and the monodentate form appears as the key intermediate.
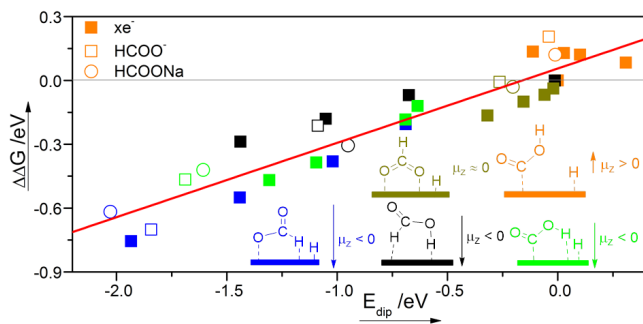
Figure 2. Scaling relation ($R^2 = 0.88$) between the change in adsorption Gibbs free energy (referenced to the non-promoted case) of five species along the pathways and the electrostatic interaction ($-\varepsilon\mu_z$) produced by the electrostatic field induced by the various promoter models. Promoter models are HCOO$^-$ anion and HCOONa, over Pd(111) and negative surface charges including 0.30, 0.50, 0.75 and 1.0e$^-$. Species along the pathway include HCOOH (black), COOH (orange), COOH (light green) and monodentate (blue) and bidentate (dark green) HCOO intermediates. The associated surface dipole moments are shown, and the electric field produced by the anionic promoters is negative. If dipole and electric field vectors are parallel, the electrostatic interaction is attractive.

The evidenced promoting effect of the electric field for the charged surface is reminiscent of an electro-promoted catalyst as discovered by Vayenas and co-workers (where the chemical process is assisted by an electrochemical potential, with the current not being involved in the main reaction)[28],[30] or an electrochemical reaction. However, HCOONa is a chemical promoter. Indeed, the chemical promotion through an adsorbate investigated herein is operationally different and complementary to these two alternatives: First of all, there is no electrical current involved, since the promotional effect is only derived from co-adsorption of chemical species from the solution. Second, in electrochemistry, the negative surface charge would be translated to a reducing potential (see Figure S7 and Table S9).[31] However, the electro-oxidation of formic acid into CO_2 and 2(H$^+$, e$^-$) is thermodynamically not possible at these potentials. In other words, in agreement with the observations in ref 31, the chemical steps in the electro-oxidation of formic acid would be slowed down by the overpotentials, necessary to obtain practical current densities.

In conclusion, in the HCOOH decomposition catalysed by Pd, the active catalyst is not the neutral metal surface, but the metal electronically enriched by the adsorption of formate anions. The generated electric field strongly facilitates the direct formate/carboxyl dehydrogenation and can be modelled by a surface charge counterbalanced by an implicit electrolyte. Our results shed new lights on the promotional effect of solution species in heterogeneous catalysis at the solid-liquid interface, providing a common framework to understand electrochemical promotion and promotions due to interactions between ionic species and metal nano-particles.

ASSOCIATED CONTENT

AUTHOR INFORMATION

Corresponding Author

* G.F.: Tel, +86-13625012808; Email: gfu@xmu.edu.cn; * P.S.: Tel, 1-310-825-8485; Email: sautet@ucla.edu

Author Contributions

The manuscript was written through contributions of all authors. / All authors have given approval to the final version of the manuscript. / $^+$P.W. and S.N.S. contributed equally.

REFERENCES

(1) Zhu, Q.-L.; Xu, Q. *Energ. Envir. Sci.* **2015**, *8*, 478-512.
(2) Grasemann, M.; Laurenczy, G. *Energ. Envir. Sci.* **2012**, *5*, 8171-8181.
(3) Hill, S. P.; Winterbottom, J. M. *J. Chem. Tech. Biotechnol.* **1988**, *41*, 121-133.
(4) Zhu, Q.-L.; Tsumori, N.; Xu, Q. *J. Am. Chem. Soc.* **2015**, *137*, 11743-11748.
(5) Jiang, K.; Xu, K.; Zou, S.; Cai, W.-B. *J. Am. Chem. Soc.* **2014**, *136*, 4861-4864.
(6) Wang, X.; Qi, G.-W.; Tan, C.-H.; Li, Y.-P.; Guo, J.; Pang, X.-J.; Zhang, S.-Y. *Int. J. Hydrogen Energ.* **2014**, *39*, 837-843.
(7) Joo, J.; Uchida, T.; Cuesta, A.; Koper, M. T. M.; Osawa, M. *J. Am. Chem. Soc.* **2013**, *135*, 9991-9994.
(8) Gao, Y.-Y.; Tan, C.-H.; Ye-Ping, L. I.; Guo, J.; Zhang, S.-Y. *Int. J. Hydrogen Energ.* **2012**, *37*, 3433-3437.
(9) Brimaud, S.; Solla-Gullón, J.; I. Weber, Feliu,J. M.; Behm, R. J. *ChemElectroChem* **2014**, *1*, 1075-1083.
(10) Perales-Rondón, J. V.; Herrero, E.; Feliu, J. M. *Electrochim. Acta* **2014**, *140*, 511-517.
(11) Davis, J. L.; Barteau, M. A. *Surf. Sci.* **1991**, *256*, 50-66.
(12) Tang, Y.; Roberts, C. A.; Perkins, R. T.; Wachs, I. E. *Surf. Sci.* **2016**, *650*, 103-110.
(13) Miyake, H.; Okada, T.; Samjeske, G.; Osawa, M. *Phys. Chem. Chem. Phys.* **2008**, *10*, 3662-3669.
(14) Yoo, J. S.; Abild-Pedersen, F.; Nørskov, J. K.; Studt, F. ACS Catal. **2014**, *4*, 1226-1233.
(15) Herron, J. A.; Scaranto, J.; Ferrin, P.; Li, S.; Mavrikakis, M. *ACS Catal.* **2014**, 4434-4445.
(16) Wang, H.-F.; Liu, Z.-P. *J. Phys. Chem. C* **2009**, *113*, 17502-17508.
(17) Chen, Y. X.; Heinen, M.; Jusys, Z.; Behm, R. J. *Langmuir* **2006**, *22*, 10399-10408.
(18) Nørskov, J. K.; Bligaard, T.; Rossmeisl, J.; Christensen, C. H. *Nat Chem* **2009**, *1*, 37-46.
(19) van Santen, R. A.; Sautet, P. in *Computational Methods in Catalysis and Materials Science*, Wiley-VCH Verlag GmbH & Co.

KGaA, 2009, pp. 1-455.

(20)   Mortensen, J. J.; Hammer, B.; Nørskov, J. K. *Phys. Rev. Lett.* **1998**, *80*, 4333-4336.

(21)   Logadóttir,Á.; Nørskov, J. K. *J. Catal.* **2003**, *220*, 273-279.

(22)   Mathew, K.; Sundararaman, R.; Letchworth-Weaver, K.; Arias, T. A.; Hennig, R. G. *J. Chem. Phys.* **2014**, *140*, 084106.

(23)   Mathew, K.; Hennig, R. G. *arXiv.org, e-Print Arch., Condens. Matter* **2016**, 1601.03346.

(24)   Steinmann, S. N.; Sautet, P., *J. Phys. Chem. C* **2016**, *120(10)*, 5619.

(25)   Kozuch, S.; Shaik, S. *Accounts Chem. Res.* **2011**, *44*, 101-110.

(26)   Zhang, R.; Liu, H.; Wang, B.; Ling, L. *J. Phys. Chem. C* **2012**, *116*, 22266-22280.

(27)   Luo, Q.; Feng, G.; Beller, M.; Jiao, H. *J. Phys. Chem. C* **2012**, *116*, 4149-4156.

(28)   Pacchioni, G.; Illas, F.; Neophytides, S.; Vayenas, C. G. *The J. Phys. Chem.* **1996**, *100*, 16653-16661.

(29)   Jones, S.; Qu, J.; Tedsree, K.; Gong, X.-Q.; Tsang, S. C. E. *Angew. Chem.* **2012**, *124*, 11437-11440.

(30) Vayenas, C. G.; Brosda, S. *Top. Catal.* **2014**, *57*, 1287-1301;

(31)   Steinmann, S. N.; Michel, C.; Schwiedernoch, R.; Filhol, J.-S.; Sautet, P. *ChemPhysChem* **2015***, 16*, 2307-2311.

Authors are required to submit a graphic entry for the Table of Contents (TOC) that, in conjunction with the manuscript title, should give the reader a representative idea of one of the following: A key structure, reaction, equation, concept, or theorem, etc., that is discussed in the manuscript. Consult the journal's Instructions for Authors for TOC graphic specifications.
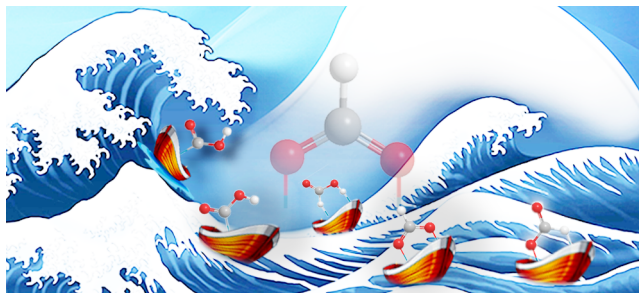
Insert Table of Contents artwork here